A Numerical-Substructure-Based Approach for the Synthesis of Substructurability and Exact Synchronisation Controllers

J.Y. Tu & J.Y. Jiang
Advanced Control and Dynamic Test Laboratory, Department of Power Mechanical Engineering, National Tsing Hua University, Taiwan

SUMMARY:
An innovative numerical-substructure-based framework for the synthesis of substructured dynamics, substructurability, and exact synchronisation controllers using state-space techniques is presented in this paper. The proposed linear substructuring controllers require no *a priori* information of the specimen dynamics, and are suitable for nonlinear testing tasks. Controllability matrices and condition numbers are introduced to analyse substructuring controllability and sensitivity. Exact synchronisation theory proposes that both the transient and steady responses of the numerical and physical substructures need to be equivalent. Experimental results explicitly show that the substructured eigenvalue techniques provide more general indications to control stability and accuracy, leading to the development of effective, efficient and successful substructuring for testing new engineering systems.

Keywords: substructuring, substructurability, substructured eigenvalues, state-space techniques, controllability

1. INTRODUCTION

Experimental dynamically substructured system (DSS) techniques are widely used in the testing of new automobiles, aircraft, and civil engineering systems, which decompose a complete dynamic system (emulated system, Σ_E) into a number of sub-components. Critical components are physically tested at full-size as physical substructure (Σ_P) and the remaining components are simultaneously simulated in real time as numerical substructure (Σ_N). High-quality control is required to synchronise the responses of the physical and numerical components and to compensate for additional dynamics introduced by actuator (transfer) systems within Σ_P.

Typically, the development of emulated-system-based (EB) DSS controllers requires knowing the nominal parameters of the tested specimen(s) prior to the tests. Examples of EB control approaches are addressed as follows. Knowledge of the entire structure is required for the design of a linear controller; see Eqns. 3. and 5. in Neild et al. (2005); an emulator is tailored to model the inverse dynamics of the actuator (Gawthrop et al., 2008), requiring the Σ_N and Σ_P transform models. However, in practice, the specimens or emulated system may contain new, nonlinear, uncertain, and unexpected dynamics. Thus, the nominal model of the specimen can be invalid or even *unavailable*, rendering the EB controllers and substructuring tests ineffective.

An innovative numerical-substructure-based (NB) framework for the synthesis of substructured dynamics and control systems are presented in this work, which uses the on-line signals and parameters related to Σ_N and the transfer systems (G_{TS}) only. Accordingly, the advantages of the NB substructuring strategies are summarised as follows: (i) *a priori* information of the tested specimen is not required; (ii) transfer-function and state-space (SS) techniques can be used to tailor control systems in a systematic manner (this paper focuses on the SS form); (3) when the Σ_N dynamics are relatively simple and include fast substructured eigenvalues, the NB controllers can be used in order to achieve exact synchronised responses. Further information about EB and NB frameworks can be referred to Tu (2012).

The concept of substructurability was first proposed by Neild et al. (2005), and this paper specifically uses the NB framework and SS-based techniques to determine the suitability of $\{\Sigma_N, G_{TS}\}$, leading to a preliminary investigation into substructurability. When the inherent dynamic properties of $\{\Sigma_N, G_{TS}\}$ are ill-conditioned or sensitive to uncertainties, the resulting substructuring which is effective in simulation may become sluggish in implementation, independent of numerical algorithms and controller designs. Furthermore, synchronisation condition is discussed in order to assess the control performance. Substructurability and synchronisation analysis would be essential prior to implementation, in order to establish effective, efficient and accurate DSS tests.

The rest of this paper is structured as follows. In Section 2, the proposed NB framework, substructured dynamics, and control systems will be presented using SS techniques. Theoretical substructurability and synchronisation analysis are introduced in Section 3. In Section 4, a one-mass-two-spring DSS is developed to experimentally verify the proposed concepts in Sections 2 and 3. Finally, conclusion is provided in Section 5.

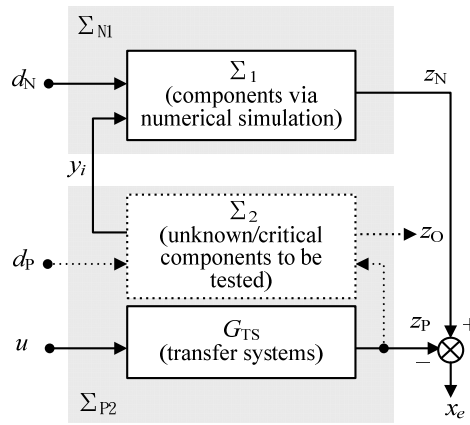## 2. THE DEVELOPMENT OF NUMERICAL-SUBSTRUCTURE-BASED SUBSTRUCTURED SYSTEMS

Figure 1. The proposed numerical-substructure-based substructured framework

2.1. NB substructured frameworks in state-space form

A numerical-substructure-based (NB) framework is presented in Fig. 1, which decomposes a complete Σ_E into at least two substructures: $\{\Sigma_1, \Sigma_2\}$. Without loss of generality, $\Sigma_N = \Sigma_1 = \Sigma_{N1}$ is the numerical substructure, Σ_2 is the tested specimen, and the transfer system is represented by G_{TS}; thus, the physical substructure is $\Sigma_{P2} = \Sigma_2 + G_{TS}$. The excitation signal is denoted by d_N if it is imposed on Σ_1 numerically, and d_P represents the physical excitation signal imposing on Σ_2. Here, d_N/d_P can be seismic forces or displacements, for example. A dynamic constraint signal is denoted by y_i, which is measured from Σ_P and fed back to Σ_N.

Signals $\{z_N, z_P\}$ in Fig. 1 indicate the responses of Σ_N and Σ_P at the substructured interface, to be synchronised via the action of a robust outer-loop DSS control signal, denoted as u. A high-fidelity DSS controller can ideally drive the substructured error to zero ($x_e = z_N - z_P$, $x_e \to 0$), towards the success of DSS testing. Signal z_O represents other critical responses to be observed or recorded, in addition to $\{y_i, z_P\}$. Note that Σ_N and/or Σ_P can contain more than one substructure, i.e., multi-input/multi-output (MIMO) systems, such that the signals $\{d_N, d_P, u, y_i, x_e, z_O, z_N, z_P\}$ can be vectors.

Since the primary purpose of DSS is to identity the critical component in Σ_2, its parameters should be assumed to be *unknown* (depicted by dotted lines). In this manner, the proposed NB framework only

considers the signals and parameters associated with $\{\Sigma_N, G_{TS}\}$ for the synthesis of DSS dynamics and controllers. The assumptions underlying the NB framework are: (a) the equations of motion in Σ_1 can be transformed into SS models (numerical algorithms are not discussed herein); (b) the Σ_2 dynamics are *unknown*; (c) G_{TS} together with its proprietary controller has a SS realisation (assuming that the delay dynamics can be matched by a Padè approximant). Accordingly, the nominal models and outputs of Σ_{N1} can be expressed by

$$\Sigma_{N1}: \begin{bmatrix} \dot{x}_{N1} \\ \hdashline \dot{x}_{N2} \end{bmatrix} = \underbrace{\begin{bmatrix} A_{N11} & A_{N12} \\ \hdashline A_{N21} & A_{N22} \end{bmatrix}}_{A_N} \begin{bmatrix} x_{N1} \\ \hdashline x_{N2} \end{bmatrix} + \underbrace{\begin{bmatrix} B_{Ni1} \\ \hdashline B_{Ni2} \end{bmatrix}}_{B_{Ni}} y_i + \underbrace{\begin{bmatrix} B_{Nd1} \\ \hdashline B_{Nd2} \end{bmatrix}}_{B_{Nd}} d_N; \quad z_N = x_{N1} = \underbrace{\begin{bmatrix} I & 0 \end{bmatrix}}_{C_N} \begin{bmatrix} x_{N1} \\ x_{N2} \end{bmatrix} \quad (2.1)$$

In Eqn. 2.1, A_N and C_N are the plant and output matrices of Σ_{N1}, respectively; $\{B_{Ni}, B_{Nd}\}$ are the input matrices for $\{y_i, d_N\}$; x_{N1} is the synchronised subset of the state of Σ_{N1} and x_{N2} is the remainder of the state. Therefore, the synchronised state of Σ_{N1} can be extracted from Eqn. 2.1 as follows

$$\dot{x}_{N1} = A_{N11}x_{N1} + A_{N12}x_{N2} + B_{Ni1}y_i + B_{Nd1}d_N \quad (2.2)$$

Similarly, assuming that a higher-order model of (MIMO) G_{TS} is identified, the output dynamics of Σ_{P2} yield

$$\Sigma_{P2} \text{ (only } G_{TS}): \begin{bmatrix} \dot{x}_{P1} \\ \hdashline \dot{x}_{P2} \end{bmatrix} = \underbrace{\begin{bmatrix} A_{P11} & A_{P12} \\ \hdashline A_{P21} & A_{P22} \end{bmatrix}}_{A_P} \begin{bmatrix} x_{P1} \\ \hdashline x_{P2} \end{bmatrix} + \underbrace{\begin{bmatrix} B_{Pu1} \\ \hdashline B_{Pu2} \end{bmatrix}}_{B_{Pu}} u; \quad z_P = x_{P1} = \underbrace{\begin{bmatrix} I & 0 \end{bmatrix}}_{C_P} \begin{bmatrix} x_{P1} \\ x_{P2} \end{bmatrix} \quad (2.3)$$

where $\{A_P, B_{Pu}, C_P\}$ are the plant, input, and output matrices, respectively. In addition, x_{P1} is the G_{TS} state to be synchronised with x_{N1}, and x_{P2} in general contains the remaining state of G_{TS}, irrelevant to the Σ_2 states. In the rest of this paper, G_{TS}, together with its inner-loop controller, is approximated by a first-order model without a loss of generality. Thus, $\{x_{P2}, A_{P12}, A_{P21}, A_{P22}, B_{Pu2}\}$ are removed and the output dynamics of Σ_{P2} become

$$\Sigma_{P2} \text{ (only } G_{TS}): \quad \dot{x}_{P1} = A_{P11}x_{P1} + B_{Pu1}u \quad (2.4)$$

As a result, subtracting Eqn. 2.4. from Eqn. 2.2., adding and subtracting $A_{P11}x_{N1}$ yields the first type of NB substructured error dynamics

$$\underbrace{\dot{x}_e = A_{P11}x_e}_{\text{(homogenous eqn.)}} + (A_{N11} - A_{P11})x_{N1} + A_{N12}x_{N2} + B_{Ni1}y_i + \underbrace{(-B_{Pu1})}_{B_u}u + B_{Nd1}d_N \quad (2.5)$$

Similarly, adding and subtracting $A_{N11}x_{P1}$ results in the second type of NB error equation

$$\underbrace{\dot{x}_e = A_{N11}x_e}_{\text{(homogenous eqn.)}} + A_{N12}x_{N2} + (A_{N11} - A_{P11})x_{P1} + B_{Ni1}y_i + \underbrace{(-B_{Pu1})}_{B_u}u + B_{Nd1}d_N \quad (2.6)$$

It will be shown in Section 3.2 that the two error equations are output-equivalent, but do not have dynamic equivalence, due to the distinct plant matrices of A_{N11} and A_{P11}. A successful DSS controller must be able to drive the error dynamics to approach zero in a fast, stable, and robust manner.

2.2. NB state-space linear substructuring controllers

The state-based strategy is adopted for substructuring control. Considering the error expressions in Eqns. 2.5. and 2.6., the solution is suggested by using a two-degree-of-freedom control policy (Skogestad and Postlethwaite, 2005), with a feedforward controller for disturbance rejection and a

feedback controller for output regulation. Hence, the first and second types of NB state-space linear substructuring controllers (N1-SSLSC and N2-SSLSC) for Eqns. 2.5 and 2.6 are proposed as

$$N1 - SSLSC: \quad u = K_{N1}x_{N1} + K_{N2}x_{N2} + K_i y_i + K_{dN}d_N + K_{en}x_e \tag{2.7}$$

$$N2 - SSLSC: \quad u = K_{N2}x_{N2} + \underline{K_{P1}x_{P1}} + K_i y_i + K_{dN}d_N + K_{en}x_e \tag{2.8}$$

where $\{K_{N1}, K_{N2}, K_i, K_{dN}\}$ and $\{K_{N2}, K_{P1}, K_i, K_{dN}\}$ are classified as feedforward gain matrices and K_{en} are feedback gain matrices. Strictly speaking, the feedforward N2-SSLSC controller is no longer an open-loop control policy, because the K_{P1} gain associating with x_{P1} is essentially a closed-loop scheme and this design will change the G_{TS} dynamic properties; see further discussion in Section 3.2. Substituting Eqns. 2.7. and 2.8 into 2.5. and 2.6., respectively, the homogeneous nature of the error dynamics are ensured via the following choice of gains

$$N1 - SSLSC: \quad K_{N1} = B_{Pu1}^{-1}\left(A_{N11} - A_{P11}\right); \quad K_{N2} = B_{Pu1}^{-1}A_{N12};$$
$$K_i = B_{Pu1}^{-1}B_{Ni1}; \quad\quad\quad K_{dN} = B_{Pu1}^{-1}B_{Nd1} \tag{2.9}$$

$$N2 - SSLSC: \quad K_{N2} = B_{Pu1}^{-1}A_{N12}; \quad K_{P1} = B_{Pu1}^{-1}\left(A_{N11} - A_{P11}\right);$$
$$K_i = B_{Pu1}^{-1}B_{Ni1}; \quad\quad K_{dN} = B_{Pu1}^{-1}B_{Nd1} \tag{2.10}$$

These feedforward gains can cancel the unwanted error dynamics in Eqns. 2.5. and 2.6., when the G_{TS} parameters are exactly known. In the presence of G_{TS} uncertainty, the closed-loop stability and robustness are ensured via the design of K_{en}, for instance, using the robust eigenstructure assignment technique (Kautsky and Nichols, 1985). Note that although the two controllers yield very similar parametric expressions, the resulting performance will be shown to be different. The NB framework is transformed into a proper control block diagram in Fig. 2, using the N1-SSLSC as an example, where Σ_2 is not included in the primary feedback control loop. Further discussion about Fig. 2 can be referred to Tu (2012).
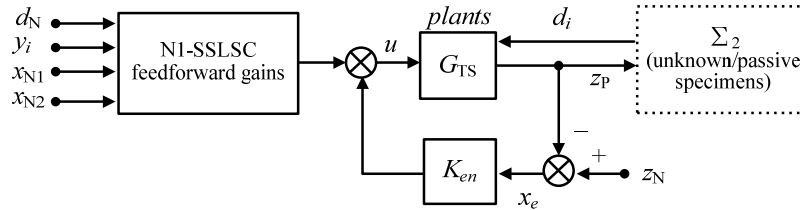

Figure 2. The proposed N1-SSLSC control block diagram

3. INTRODUCTION TO SUBSTRUCTURABILITY AND EXACT SYNCHRONISATION

3.1. Substructurability

Substructurability is proposed to be defined prior to controller design and implementation, for the purpose of promoting the control and test efficiency. This paper suggests SS-based and computer-based methods to analyse $\{\Sigma_N, G_{TS}\}$, in terms of their state controllability, stability, sensitivity, and transient performance as a whole, in order to define substructurability in a systematic and transparent manner. These inherent dynamic properties are investigated by looking at their controllability matrices, eigenvalues, and condition numbers, which can be computed via the Matlab function routines, *ctrb*, *rank*, *eig*, and *cond*. When the efficiency is approved, the exact synchronisation theory in Section 3.2 gains a deeper understanding of the synchronisation conditions for knowing how to improve the control and test accuracy.

Controllability matrices are determined using the plant and input matrices of the state equations, which need to be of full rank, such that a feedback controller can be designed. Eigenvalues (denoted by eig) are precisely the poles of a system in the transform description, indicating stability and frequency-dependent behaviour, including settling time and damping response. For stable and fast transient characteristics, the (dominative) eigenvalues must stay in deviation to the left in the s-plane, as shown in Fig. 3. When the eig is near to the image axis, degraded or unstable response can happen during a test. Condition number is defined as the ratio between the maximum and minimum singular values of a matrix (Skogestad and Postlethwaite, 2005). Generally speaking, a large condition number or an ill-conditioned plant matrix implies sensitivity to input uncertainty (Freudenberg and Loose, 1985) or reduced efficacy of model-inverse-based controllers (Skogestad and Postlethwaite, 2005). Namely, small perturbation within the input vector or plant model can change the solution vector significantly. The technique of condition number is used in particular for multivariable, second and higher-order systems, providing with a quantitative input-output controllability index. Typically, the condition number with a value of one indicates optimal input-output properties of the plant matrix.
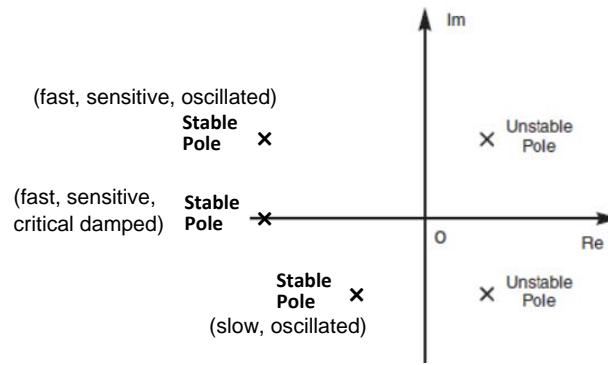

Figure 3. Stability, performance, and sensitivity related to substructured eigenvalues (Chen et al., 2009)

Therefore, a suitable design of $\{\Sigma_{N1}, G_{TS}\}$ resulting in well-conditioned substructurability as well as efficient tests should possess the properties of a full-rank controllability matrix, appropriate locations of eigenvalues, and small condition numbers (denoted by cond). A general procedure to determine substructurability is introduced as follows.

Given the expressions of Eqns. 2.5. and 2.6., the state controllability can be determined using the matrices $\{A_{P11}, B_u\}$ and $\{A_{N11}, B_u\}$, respectively. The controllability matrices are written as

$$\left[B_u \mid A_{P11}B_u \mid A_{P11}{}^2 B_u \mid \cdots \mid A_{P11}{}^{n-1}B_u \right] \tag{2.11}$$

$$\left[B_u \mid A_{N11}B_u \mid A_{N11}{}^2 B_u \mid \cdots \mid A_{N11}{}^{n-1}B_u \right] \tag{2.12}$$

Here, B_u is a square $n \times n$ matrix, as the dimension of x_e equals that of u. The controllability matrices in Eqns. 2.11. and 2.12. which have full-rank n indicate controllable DSSs.

In terms of eigenvalue techniques, faster actuation related to G_{TS} can be observed if eig(A_P) is in deviation to the left. Furthermore, *substructured eigenvalues*, which dictate the dynamic properties of the substructured errors, are proposed in this paper. For example, the substructured eigenvalues are defined as eig(A_{N11}) and eig(A_{P11}) from Eqns. 2.5. and 2.6., respectively, which dominate the x_e stability and decaying rate. To be noted that, having proper conditions for eig(A_N) or eig(A_P) does not necessarily reflect appropriate eig(A_{N11}) or eig(A_{P11}) for substructuring tests. In addition, it will be shown in Section 3.2 that, to pursue exact synchronisation performance, stable eig(A_{N11}) is necessary.

On the other hand, sensitivity conditions of first-order Σ_{N1}/G_{TS} can be evaluated by knowing the location of eig(A_N)/eig(A_P). For higher-order Σ_{N1}/G_{TS} models, cond(A_N)/cond(A_P) are considered for the sensitivity analysis. In general, faster eig and large cond would imply that sensitive simulation

within Σ_N is perturbed by y_i, or sensitive control to model mismatch, coupled dynamics, and signal noises within G_{TS} can severely lead to inaccurate responses.

3.2. Exact synchronisation

Synchronisation accuracy associated with the control design is discussed, and the definition of dynamic and output responses is introduced first. In this paper, the *dynamic properties* associated with transient state is twofold: (1) eigenvalues characterise the settling and damping responses and (2) condition numbers indicate the sensitivity to disturbance signals. Furthermore, the *output properties* specifically mean the (tracking) performance in steady state after the transient. Variant controllers can result in output equivalent and ensure zero tracking error in steady state; however, they may yield different dynamic properties, e.g. slow or fast settling period. Therefore, the N1-SSLSC and N2-SSLSC-controlled synchronisation accuracy associated with the dynamic and output properties are discussed as follows.

Firstly, the feedforward gains of Eqns. 2.9. and 2.10. are substituted into the corresponding control equations in Eqns. 2.7 and 2.8. Then, substitution of the control equations into Eqn. 2.4 enables the controlled G_{TS} dynamics to be expressed by ($K_{en} = 0$)

$$\text{N1} - \text{SSLSC}: \quad \underline{\dot{x}_{P1} = A_{P11}x_{P1} + \left(A_{N11} - A_{P11}\right)x_{N1} + A_{N12}x_{N2} + B_{Ni1}y_i + B_{Nd1}d_N} \approx \underline{\dot{x}_{N1}} \qquad (2.13)$$

$$\text{N2} - \text{SSLSC}: \quad \underline{\dot{x}_{P1} = \left(A_{P11} + A_{N11} - A_{P11}\right)x_{P1} + A_{N12}x_{N2} + B_{Ni1}y_i + B_{Nd1}d_N}$$
$$= A_{N11}x_{P1} + A_{N12}x_{N2} + B_{Ni1}y_i + B_{Nd1}d_N = \underline{\dot{x}_{N1}}_{\text{exact}} \qquad (2.14)$$

Assuming that the G_{TS} parameters are exactly known and G_{TS} is under perfect feedforward control, such that x_{P1} approaches x_{N1} and $x_e \to 0$, N2-SSLSC can achieve output and dynamic equivalences between G_{TS} and Σ_{N1} in both steady and transient states, showing *exact synchronisation* and requiring stable eig(A_{N11}). In contrast, the feedforward N1-SSLSC controller can only yield $x_{P1} \approx x_{N1}$, i.e. output equivalence in steady state and dynamic inequivalence in transient state. The output and dynamic equivalences associated with the feedback controller, K_{en}, will be discussed in the future work.

It is noted from Eqn. 2.14 that the N2-SSLSC-K_{P1} gain has shifted (part of) the poles of G_{TS} to new locations, i.e., eig(A_{P11}) is moved to eig(A_{N11}). This feedforward and model-inverse gain essentially exhibits a closed-loop or feedback control policy. When eig(A_{N11}) is near to the image axis or is marginally stable, such a dynamics-shifting condition would be disadvantageous and the synchronisation performance would be degraded during a test.

4. IMPLEMENTATION STUDIES

To practically demonstrate the concepts of the NB controllers, a one-mass-two-spring (OMTS) DSS is developed. Section 4.1 derives the NB substructured dynamics, leading to the design of N1-SSLSC and N2-SSLSC. Synchronisation performances of the two controllers are compared in Section 4.2 via experiments. A discussion of the testing results is provided in Section 4.3.

In Fig. 4(a) the dotted line represents the substructured interface, and Σ_E is decomposed into two subsystems: Σ_1: $\{m, k_1, c\}$ and Σ_2: $\{k_2\}$. Here, Σ_1 is modelled numerically and Σ_2 is tested physically, as shown in Fig. 4(b). Fig. 5 displays the Σ_{P2} test rig, where one end of the spring is connected to an electric actuator (G_{TS}), and the other is rigidly fixed, such that $\Sigma_{P2} = \Sigma_2 + G_{TS}$. The numerical excitation signal is denoted as d_N; the interaction force f_P is measured from the load cell and fed back to Σ_{N1}, acting as the constraint signal. Hence, the displacement output of Σ_{N1}, $z_N = x_{N1}$, must be synchronised with the G_{TS} output, $z_P = x_{P1}$, via the action of the NB controllers. Table 1 summarises the nominal parameters of $\{\Sigma_{N1}, G_{TS}\}$.
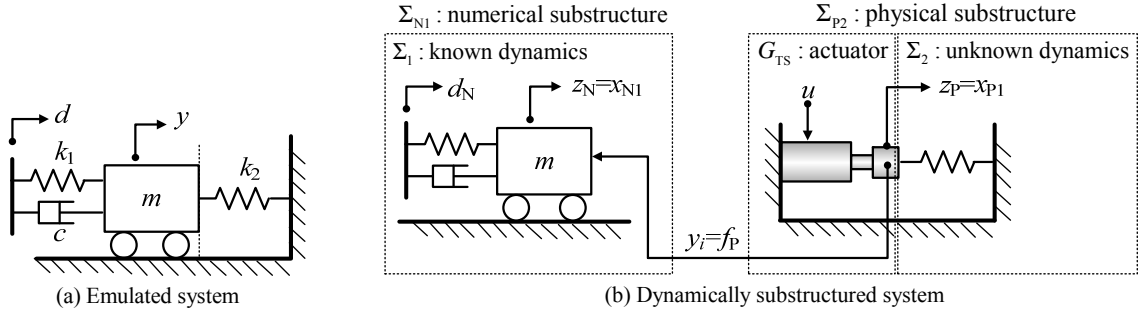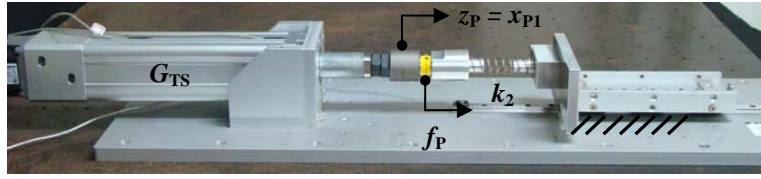
Figure 4. The one-mass-two-spring system

Figure 5. The physical substructure and testing rig

Table 1. Notation and parameter for the TMS DSS

Parameter	Description	Value
m	Mass	10 kg
k_1	Spring constant	1800 N/m
c	Viscous friction coefficient	100 Ns/m
k_2	Spring constant	unknown
$\{a, b\}$	Nominal actuator numerator and denominator coefficients	$\{48.6, 49.2\}\text{s}^{-1}$

4.1. The NB substructured frameworks and controller designs

From Fig. 4(b), the equation of motion of m in Σ_{N1} is expressed by

$$m\ddot{z}_N = k_1\left(d_N - z_N\right) + c\left(\dot{d}_N - \dot{z}_N\right) - f_P \tag{2.15}$$

Therefore, the SS model for Σ_{N1} can be derived as follows

$$\begin{bmatrix} \dot{x}_{N1} \\ \dot{x}_{N2} \end{bmatrix} = \underbrace{\begin{bmatrix} \frac{-c}{m} & 1 \\ \frac{-k_1}{m} & 0 \end{bmatrix}}_{A_N}\begin{bmatrix} x_{N1} \\ x_{N2} \end{bmatrix} + \underbrace{\begin{bmatrix} 0 \\ \frac{-1}{m} \end{bmatrix}}_{B_{Ni}}\underbrace{f_P}_{y_i} + \underbrace{\begin{bmatrix} \frac{c}{m} \\ \frac{k_1}{m} \end{bmatrix}}_{B_{Nd}}d_N; \quad z_N = \underbrace{\begin{bmatrix} 1 & 0 \end{bmatrix}}_{C_N}\begin{bmatrix} x_{N1} \\ x_{N2} \end{bmatrix} \tag{2.16}$$

where $x_{N1} = z_{N1}$ is the synchronised output. Furthermore, a first-order model of G_{TS} is identified as

$$\dot{x}_{P1} = \underbrace{(-a)}_{A_P = A_{P11}} x_{P1} + bu; \quad z_P = x_{P1} \tag{2.17}$$

Thus, extracting $\dot{x}_{N1}$ from Eqn. 2.16., subtracting $\dot{x}_{P1}$ from $\dot{x}_{N1}$, and adding and subtracting $A_{P11}x_{N1}$ or $A_{N11}x_{P1}$ result in the two types of substructured error equation

$$\dot{x}_e = \dot{x}_{N1} - \dot{x}_{P1} = \underbrace{(-a)}_{A_{P11}} x_e + \underbrace{\left(-\frac{c}{m} + a\right)}_{A_{N11} - A_{P11}} x_{N1} + \underbrace{1}_{A_{N12}} x_{N2} + \underbrace{\left(\frac{c}{m}\right)}_{B_{Nd1}}d_N + \underbrace{(-b)}_{B_u}u \tag{2.18}$$

$$\dot{x}_e = \dot{x}_{N1} - \dot{x}_{P1} = \underbrace{\left(\frac{-c}{m}\right)}_{A_{N11}} x_e + \underbrace{\frac{1}{-}}_{A_{N12}} x_{N2} + \underbrace{\left(-\frac{c}{m}+a\right)}_{A_{N11}-A_{P11}} x_{P1} + \underbrace{\left(\frac{c}{m}\right)}_{B_{Nd1}} d_N + \underbrace{(-b)}_{B_u} u \tag{2.19}$$

Referring to Eqns. 2.7., 2.8., 2.18., and 2.19., the modified N1-SSLSC and N2-SSLSC control equations are proposed in Table 2, together with the control gain design and synthesis.

Table 2. Control gain design and synthesis

	N1-SSLSC	N2-SSLSC
control equation	$u = K_{N1}x_{N1} + K_{N2}x_{N2} + K_{dN}d_N + K_{en}x_e$	$u = K_{N2}x_{N2} + \underline{K_{P1}x_{P1}} + K_{dN}d_N + K_{en}x_e$
control gain design	$K_{N1} = \frac{1}{b}\left(a - \frac{c}{m}\right); \quad K_{N2} = \frac{1}{b}; \quad K_{dN} = \frac{1}{b}\left(\frac{c}{m}\right)$	$K_{N2} = \frac{1}{b}; \quad K_{P1} = \frac{1}{b}\left(a - \frac{c}{m}\right); \quad K_{dN} = \frac{1}{b}\left(\frac{c}{m}\right)$
control gain synthesis	$K_{N1} = 0.78; \quad K_{N2} = 0.02; \quad K_{dN} = 0.2$ $K_{en} = 0$	$K_{N2} = 0.02; \quad K_{P1} = 0.78; \quad K_{dN} = 0.2$ $K_{en} = 0$ and 0.78

Table 2 shows that the gain synthesis only associates with the $\{\Sigma_{N1}, G_{TS}\}$ parameters, irrespective of Σ_2, reflecting the NB scheme. The feedback gains of $K_{en} = 0$ and 0.78 were selected for implementation, enabling a comparison of feedforward and feedback control strategies. The computation of $K_{en} = 0.78$ is referred to the eigenvalue assignment (EA) techniques (Kautsky and Nichols, 1985), and therefore the resulting controller is labelled as N2-SSLSC-EA.

4.2. Implementation results

Tests were conducted on the OMTS-DSS rig in Fig. 5 in order to compare (1) the feedforward and feedback control performances, and (2) the N1-SSLSC and N2-SSLSC synchronisation performances. The electric actuator operated in the range ±50 mm and the load cell ±445 N; the DSS controllers were implemented via an outer-loop dSPACE® 1104 system, with a control sampling frequency of 10 kHz. Excitation, d_N, was chosen to be a swept sinusoid with an amplitude of 0.004 m, frequency varying from 5 to 0.1 Hz over a time span of 20 s, ramped by 3 s.

Fig. 6 shows that the three controllers have synchronised $\{x_{N1}, x_{P1}\}$ or $\{z_N, z_P\}$ satisfactorily and yielded almost identical responses. For a better indication of control performance, the integral square error (ISE) curves corresponding to Fig. 6 is provided in Fig. 7(a), where the ISE equation is given by

$$\text{ISE} = \int_0^{20} x_e^2 dt = \int_0^{20} \left(x_{N1} - x_{P1}\right)^2 dt = \int_0^{20} \left(z_N - z_P\right)^2 dt \tag{2.20}$$

When $K_{en} = 0$, N1-SSLSC outperformed N2-SSLSC, and the N1-SSLSC-ISE ended up with a value of $\sim 0.4 \times 10^{-6}$ m^{2}s. The feedback gain of $K_{en} = 0.78$ resulted in a notable improvement as regards the N2-SSLSC performance, showing the effectiveness of the feedback control gain.

Furthermore, a set of experiments to investigate the substructured eigenvalues associated with the synchronisation performance is presented in Fig. 7(b). During these tests, the values of $\{m, k_1\}$ and eig$(A_{P11}) = -48.6$ were fixed, while the viscous friction coefficient, c, varied from 100 to 1000 Ns/m, in order to model the changes of eig(A_{N11}) or eig$(-c/m)$. The changes of eig(A_{N11}) is depicted in the x-axis. Considering the N1-SSLSC performance first, with the increment of c, the displacement magnitude was reduced, however, the ISE value was promoted. In contrast, the N2-SSLSC synchronisation performance improved with the enlarged c. It is noted that, eig$(A_{N11}) = $ eig$(A_{P11}) = -48.6$ reflects an index to determine the design of substructured eigenvalues related to the controllers. N2-SSLSC outperforms N1-SSLSC when eig(A_{N11}) is faster than eig(A_{P11}). When eig(A_{N11}) is slower than eig(A_{P11}), N1-SSLSC needs to be used for achieving better synchronisation.
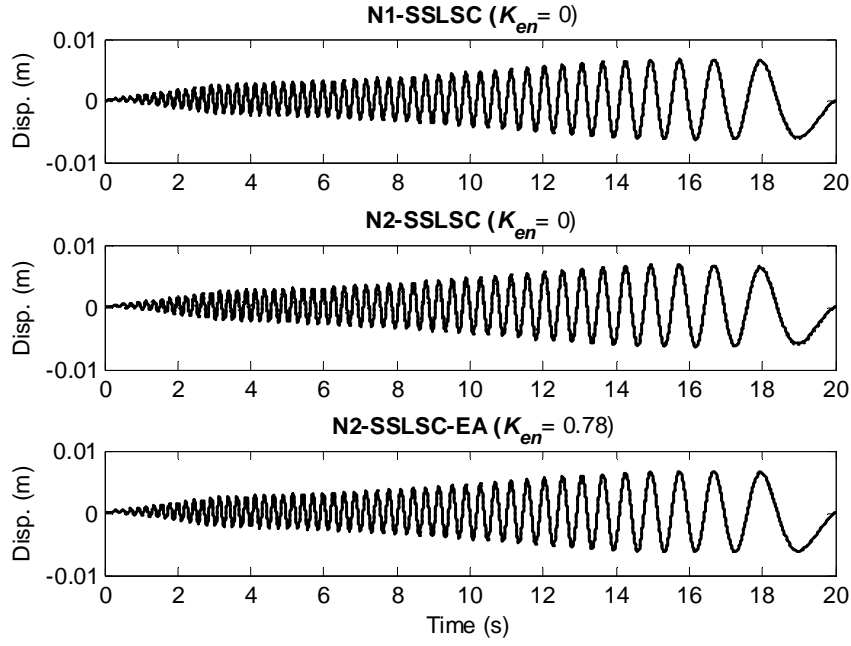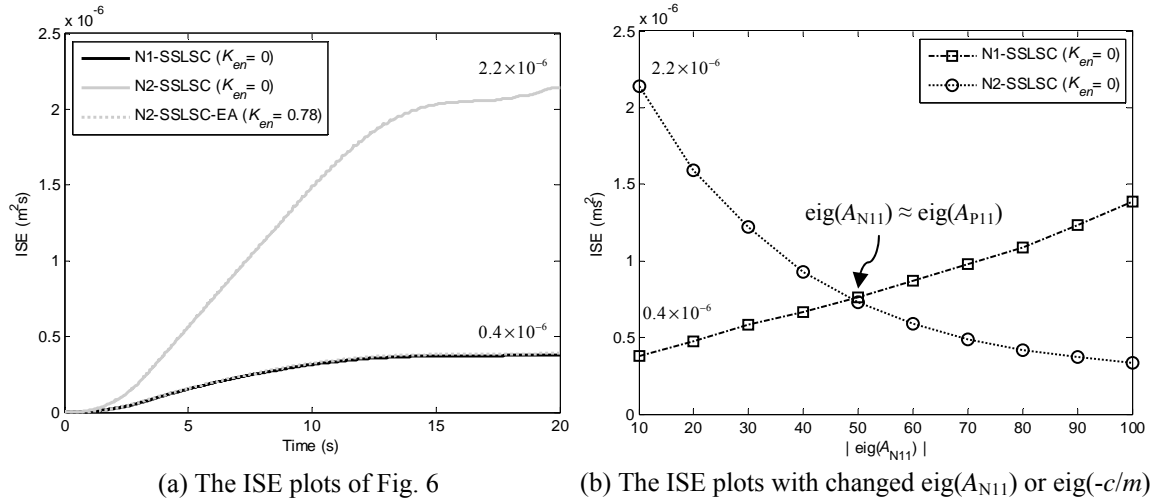
Figure 6. The experimental results with $c = 100$, the dotted line being $x_{N1} = z_N$ and the solid line being $x_{P1} = z_P$

(a) The ISE plots of Fig. 6   (b) The ISE plots with changed $\text{eig}(A_{N11})$ or $\text{eig}(-c/m)$

Figure 7. ISE curves for the experimental DSS errors

4.3. Discussion

This discussion focuses on the results of Fig. 7, which relates the substructured eigenvalues to the open and closed-loop control policies and to the exact synchronisation theories. Essentially, the design methodology of N1-SSLSC and N2-SSLSC are similar; however, they performed differently in Fig. 7, due to distinct dynamic properties related to their substructured eigenvalues. The K_{P1} gain associated with x_{P1} has transformed the N2-SSLSC ($K_{en} = 0$) to a closed-loop control scheme, shifting the G_{TS} pole from $\text{eig}(A_{P11})$ to $\text{eig}(A_{N11})$. This design slowed down the error convergence and increased the ISE values, when $\text{eig}(A_{N11})$ is near to the image axis; see the grey-solid line in Figs. 7(a). Therefore, Fig. 7(b) indicates that high quality of exact synchronisation using N2-SSLSC can only be achieved when $\text{eig}(A_{N11})$ possesses the properties of stability and fast settling time.

5. CONCLUSION

Two types of numerical-substructured-based controllers are developed and verified in this work. Experimental results in Section 4 conclude that the proposed substructured eigenvalue techniques related to numerical substructures and transfer systems is important in terms of selecting open or closed-loop control strategies, which would be independent of control algorithms. If slow substructured eigenvalues are not noticed in the control design, degraded synchronisation performance can result in, leading to inefficient and inaccurate testing results.

REFERENCES

Chen, C., Ricles, J. M., Marullo, T. M. and Mercan, O. (2009). Real-time hybrid testing using the unconditionally stable explicit CR integration algorithm. *Earthquake Engineering & Structural Dynamics* **38**:**1**, 23-44.

Freudenberg, J. S. and Loose, D. P. (1985). Relations between properties of multivariable feedback systems at different loop-breaking points: Part I. *24th IEEE Conference on Decision and Control.*

Gawthrop, P. J., Virden, D. W., Neild, S. A. and Wagg, D. J. (2008). Emulator-based control for actuator-based hardware-in-the-loop testing. *Control Engineering Practice* **16**:**8**, 897-908.

Kautsky, J. and Nichols, N. K. (1985). Robust pole assignment in linear state feedback. *International Journal of Control* **41** 1129-1155.

Neild, S. A., Stoten, D. P., Drury, D. and Wagg, D. J. (2005). Control issues relating to real-time substructuring experiments using a shaking table. *Earthquake Engineering & Structural Dynamics* **34**:**9**, 1171-1192.

Skogestad, S. and Postlethwaite, I. (2005). Multivariable feedback control: analysis and design*,* Chichester, John Wiley & Sons Ltd.

Tu, J. Y. (2012). The development of numerical-substructure-based and output-based substructuring controllers. *Structural Control and Health Monitoring*, under review.